Journal of Zhejiang University SCIENCE
ISSN 1009-3095
http://www.zju.edu.cn/jzus
E-mail: jzus@zju.edu.cn

Numerical analysis of ultimate strength of concrete filled steel tubular arch bridges

XIE Xu (谢 旭)[†1], CHEN Heng-zhi (陈衡治)[†1], LI Hui (李 辉)[2], SONG Shi-rui (宋世锐)[3]

([1]*Department of Civil Engineering, Zhejiang University, Hangzhou 310027, China*)
([2]*Department of Civil Engineering, Ningbo University, Ningbo 315211, China*)
([3]*Centre for Civil & Construction Engineering, University of Manchester, Manchester, M601QD, United Kingdom*)
[†]E-mail: xiexu@zju.edu.cn; chenhengzhi78@yahoo.com.cn

Received July 30, 2004; revision accepted Dec. 1, 2004

Abstract: The calculation of ultimate bearing capacity is a significant issue in the design of Concrete Filled Steel Tubular (CFST) arch bridges. Based on the space beam theory, this paper provides a calculation method for determining the ultimate strength of CFST structures. The accuracy of this method and the applicability of the stress-strain relationships were validated by comparing different existing confined concrete uniaxial constitutive relationships and experimental results. Comparison of these results indicated that this method using the confined concrete uniaxial stress-strain relationships can be used to calculate the ultimate strength and CFST behavior with satisfactory accuracy. The calculation results are stable and seldom affected by concrete constitutive relationships. The method is therefore valuable in the practice of engineering design. Finally, the ultimate strength of an arch bridge with span of 330 m was investigated by the proposed method and the nonlinear behavior was discussed.

Key words: Concrete Filled Steel Tubular (CFST), Confined concrete, Stress-strain relationship, Ultimate strength
doi:10.1631/jzus.2005.A0859 **Document code:** A **CLC number:** TU31

INTRODUCTION

As a result of the combined effects of the rolled steel tube and the core concrete, Concrete Filled Steel Tubular (CFST) structures can effectively take advantage of these two materials to improve the compressive strength and the ductility of the structures. This kind of structure is developing quickly in China and widely used in high-rise structures and bridges. Recently, due to the development of construction projects, numerous studies on CFST structures have been implemented by both experimental investigations and theoretical analyses (Cai, 2003; Han, 2000, Zhong, 1999). Although the behavior of CFST structures has been extensively examined, the concrete core confinement is not yet well understood.

Experimental applications of CFST arch bridges began in China in the 1990s. Based on the large numbers of CFST arch bridges built in recent decades, much valuable experience has been gained in structural design and building practice. However, owing to the late start of the engineering practice, research on the resistance to overturning and failure mechanism of the CFST structures is lacking. The current design methods take little account of the confinement effect of the steel tube ring on the concrete core, and only evaluate the structural stability by the elastic eigenvalue. The design theories of CFST arch bridges have fallen behind the corresponding fundamental research, and the up-to-date research findings still have not been applied to engineering design.

It is well known that the arch ribs are basically compression structures. The calculation of secondary stress due to the deformation of arch axis, the analysis of the geometrical nonlinear effect and the estimation of ultimate bearing capacity are all important issues of structural design. CFST arch bridges where the cross-sectional dimensions are determined by the inner forces do not always satisfy the stabilization of the CFST arch bridges. An appropriate design method

for evaluating structural stability must take into account the effects of geometrical and material nonlinearity.

The core concrete and the steel tube are in a complex 3D stress state, because the lateral deformation of concrete is bounded by the steel tube when CFST structures are compressed in the axial direction. In recent years, 3D finite element method (FEM) has been used to simulate the ultimate behavior of CFST structures (Fujii, 2003). However, to estimate the ultimate strength of CFST structures by 3D nonlinear FEM is still difficult and impractical in engineering design at present due to the following reasons: (1) The failure law and constitutive relationship of concrete in the tri-axial stress state are complex; (2) The results of calculation are largely dependent on the material parameters; (3) The amount of calculation is large.

The purpose of this study is to develop an appropriate method for evaluating the ultimate strength of CFST arch bridges. An evaluation method is put forward based on the space beam theory. As a stage of the study, an analytical approach of the method is presented and the constitutive relationship of core concrete is examined. Examples are presented to verify the accuracy of this method. Finally, the ultimate strength of an arch bridge with span of 330 m is investigated by the proposed method and the nonlinear behavior is discussed.

ANALYTICAL THEORY

Basic assumptions

To simplify the calculation, the following assumptions are adopted:

(1) A plane section originally normal to its neutral axis will always remain a plane and normal to the neutral axis during the deformation;

(2) The shear deformation due to the shear force is ignored, and the torsional deflection satisfies the St. Venant torsional theory;

(3) The shear stress affecting the stress-strain relation of the material is neglected.

Although the first assumption is not necessary, it can simplify the calculation. In addition, the first assumption can be satisfied according to the interrelated experimental results (Cai, 2003). The second and third assumptions are introduced here because the arch ribs are essentially compression structures, so the influence of shear and torsion on their ultimate strength is insignificant.

Stress-strain relation of core concrete and steel tube

In the analysis approach proposed in this paper, the accuracy of analysis depends on the uniaxial stress-strain relationships of confined concrete and steel tube material. At present, an accurate stress-strain relationship for steel tube has already been developed. Although a few models of stress-strain relationships for confined concrete have been developed (Han, 2000; Pan, 1989; Nosaki, 1996; Susantha and Ge, 2001; Tang and Hino, 1996), there are not enough comparative studies on these existing constitutive relationships of concrete under ultimate behavior, and the accuracy of these models has not been examined thoroughly.

1. Uniaxial stress-strain relationship of confined concrete

Fig.1 shows that the complete stress-strain curve of confined concrete is different from that of plain concrete. The compressive strength and the ductility are improved when concrete is confined by a surrounding steel tube.

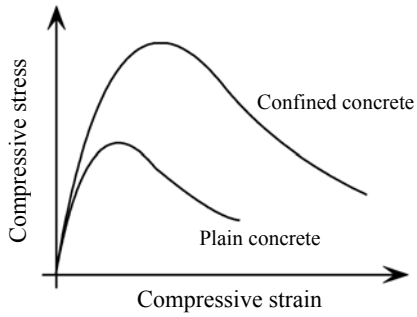

Fig.1 General stress-strain curves for confined concrete and unconfined concrete

To explore the influences of different constitutive relationships of confined concrete on the ultimate strength and behavior, the failure behaviour of CFST structures were analyzed with three different constitutive relationships and the results are compared.

The first constitutive relationship of confined concrete selected was presented by Han (2000), and the uniaxial stress-strain relation is:

$$\varepsilon \le \varepsilon_0,\ \sigma = \sigma_0 \varepsilon / \varepsilon_0 [2.0 - K - (1-K)\varepsilon / \varepsilon_0] \qquad (1a)$$

$$\varepsilon > \varepsilon_0,$$

$$\sigma=\begin{cases}\sigma_0(1-q)+\sigma_0 q(\varepsilon/\varepsilon_0)^{0.1\xi} & (\xi\geq 1.12)\\ \sigma_0(\varepsilon/\varepsilon_0)/[\beta(\varepsilon/\varepsilon_0-1)^2+\varepsilon/\varepsilon_0] & (\xi<1.12)\end{cases} \tag{1b}$$

where σ and ε are the longitudinal compressive stress and strain respectively. The other symbols are defined as follow:

$$\begin{cases}\sigma_0=f_{ck}[1.194+(13/f_{ck})^{0.45}(-0.07485\xi^2+0.5789\xi)]\\ \varepsilon_0=\varepsilon_c+[1400+40(f_{ck}-20)]\xi^{0.2}\\ \varepsilon_c=1300+14.93f_{ck}\\ K=0.1\xi^{0.745}\\ q=K/(0.2+0.1\xi)\\ \beta=5.0f_{ck}^2\times(2.36\times10^{-5})^{0.25+(\xi-0.5)^7}\times10^{-4}\\ \xi=\alpha f_y/f_{ck}\\ \alpha=A_s/A_c\end{cases} \tag{2}$$

where f_{ck} is the cubic compressive strength of concrete (MPa), A_s is the area of steel tube (m^2), A_c is the area of concrete (m^2), f_y is the yield strength of steel tube (MPa).

The second constitutive relationship selected was brought forward by Pan (1989), who gave the stress-strain relation as:

$$\varepsilon\leq\varepsilon_0,\quad \sigma=\sigma_0\varepsilon/\varepsilon_0[2.0-K-(1-K)\varepsilon/\varepsilon_0] \tag{3a}$$

$$\varepsilon>\varepsilon_0,\quad \sigma=\sigma_0(1-q)+\sigma_0 q(\varepsilon/\varepsilon_0)^{0.2+\alpha} \tag{3b}$$

in which the symbols are defined as follows:

$$\begin{cases}\sigma_0=f_c[1+(30/f_{cu})^{0.45}(-0.0626\xi^2+0.4848\xi)]\\ \varepsilon_0=\varepsilon_c+3600\sqrt{\alpha}\\ \varepsilon_c=1300+10f_{cu}\\ K=0.02(-5\alpha^2+3\alpha)(50-f_{cu})+0.02(-2\alpha^2\\ \quad+2.15\alpha)(f_{cu}-30)\\ q=K/0.2+\alpha\\ \xi=\alpha f_y/f_c\\ \alpha=A_s/A_c\\ f_c=0.8f_{cu}\end{cases} \tag{4}$$

The third constitutive relationship was presented by Nosaki (1996), who gave the stress-strain relation as:

$$\frac{\sigma}{\sigma_{c0}}=\frac{AX+(d-1)X^2}{1+(A-2)X+dX^2} \tag{5}$$

in which the symbols are defined as follows:

$$\begin{cases}d=1.5-0.0171f_{cp}+2.39\sqrt{(K-1)f_{cp}/23}\\ X=\varepsilon/\varepsilon_{c0}\\ A=E_c\varepsilon_{c0}/\sigma_{c0}\\ \sigma_{c0}=f_{cp}+8.2\alpha t f_y/(D-2t)\\ \varepsilon_{c0}=\begin{cases}\varepsilon_0[1+4.7(K-1)] & K\leq1.5\\ \varepsilon_0[3.35+20(K-1.5)] & K>1.5\end{cases}\\ \varepsilon_0=0.94f_{cp}^{0.25}\times10^{-3}\\ K=\sigma_{c0}/f_{cp}\\ f_{cp}=\varphi f_{cu}\end{cases} \tag{6}$$

where f_{ck} is the concrete cylinder compressive strength (MPa), f_{cp} is the concrete cylinder compressive strength considering the dimensional effect coefficient φ (Fig.2) (MPa), σ_{c0} is the compressive strength of core concrete (MPa), ε_{c0} is the strain corresponding to ε_{c0} ($\mu\varepsilon$), ε_0 is the strain corresponding to ultimate strength of plain concrete ($\mu\varepsilon$), D is the diameter of steel tube (m), t is the wall thickness of steel tube (m), α is σ_θ/f_y, the effective confinement coefficient of steel acting on core concrete, σ_θ is the ultimate tangential stress of steel tube (MPa).

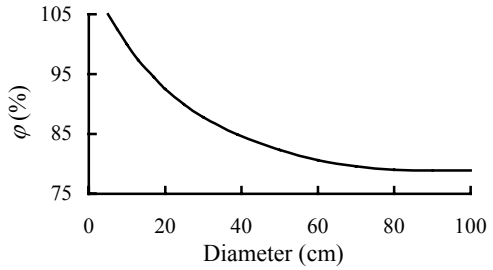

Fig.2 Influence of different structure dimensions on the strength of concrete

The Young's modulus of the concrete in Eq.(6) is expressed by the following Eq.(7):

$$E_c=\left(6.90+3.32\sqrt{\sigma_{cp}}\right)\times10^3 \tag{7}$$

Fig.3 shows a comparison of the corresponding stress-strain curves of the different constitutive rela-

tionships of the confined concrete. The strength grades of the concrete are assumed as C40 (f_{ck}=26.8 MPa) and C60 (f_{ck}=41 MPa); the diameter of steel tube varies from 50 cm to 100 cm; the steel tube wall thickness is set to 1.0 cm (thus D/t=50~100); and the steel tube yield strength is 250 MPa. In addition, the ratio of the concrete cylinder compression strength to the cubic compression strength (20×20×20 cm) is 0.80, and the influence of the structure dimensions in Eq.(5) is not taken into account for the unified standards (φ=1.0).

Fig.3 indicates that the difference between the 3 constitutive relationships is not significant in the low compressive strain range. However, the difference is obvious with the increase of strain, especially the curve calculated from Eq.(3) shows the opposite trend in the high strain range compared to the other two constitutive relationships. Although the comparison results for the lower value of D/t are not presented in Fig.3, the stress-strain curves of Eqs.(1) and (5) have a coincident trend with the reduction of D/t.

2. Uniaxial stress-strain relationship of steel tube

The interaction of the radial stress σ_r and the tangential stress σ_θ are taken into account when calculating the tensile strength and the compression strength of the steel tube. According to the Von Misess yield criterion, the yield condition under a 2D stress state is given by Eq.(8) (shown in Fig.4a):

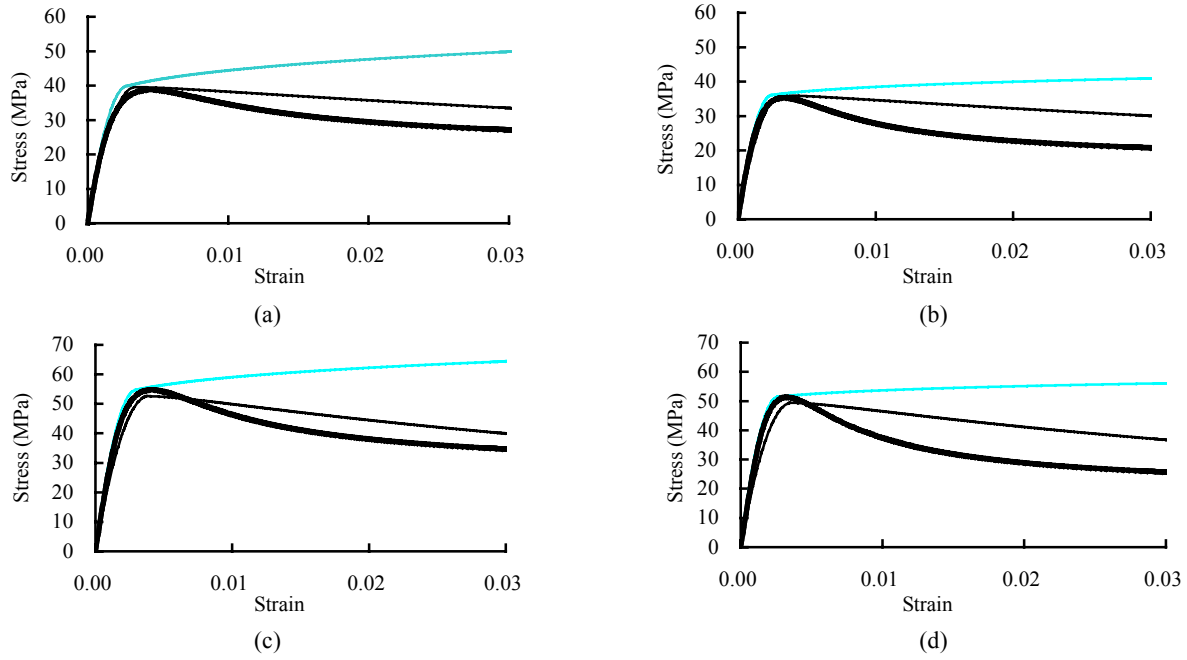

Fig.3 Comparison of different stress-strain curves of core concrete. (a) *D*=50 cm, C40; (b) *D*=100 cm, C40; (c) *D*=50 cm, C60; (d) *D*=100 cm, C60. ——— Eq.(1); ——— Eq.(3); ——— Eq.(5)

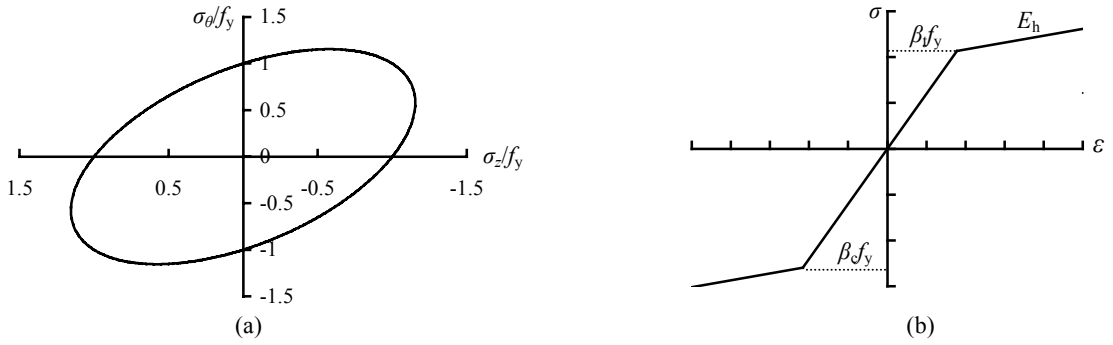

Fig.4 Stress-strain curves of steel tube. (a) Yield condition; (b) Stress-strain relationship

$$\sigma_z^2 - \sigma_z\sigma_\theta + \sigma_\theta^2 = f_y^2 \tag{8}$$

where σ_z is the steel tube axial normal stress.

If $\alpha=\sigma_\theta/f_y\approx0.159$ is substituted into Eq.(8), the tensile and compressive yield strengths are as Eq.(9):

$$\begin{cases}\sigma_{yt} = \beta_t f_y = 0.911 f_y \\ \sigma_{yc} = \beta_c f_y = 1.07 f_y\end{cases} \tag{9}$$

Eq.(9) denotes that the yield strength on the tension and compression side of the steel tube are respectively the products of β_t or β_c and the yield strength of a steel tube without core concrete. Adopting the bilinear nonlinear material model and considering hardening, the steel tube stress-strain curve can be as shown in Fig.4b.

The secondary modulus of steel tube E_h relates to both the material characteristics and local buckling. It is assumed that E_h equals 1% of the initial elastic modulus.

Fig.5 shows the symmetrical cross section of a CFST structure where O represents the centre of the cross-section. The cross-section is divided into many small fibers. If the element is sufficiently small, the element strain increment can be expressed as that of the fiber center (x_i, y_i). According to the first assumption in this paper, with the theory of Updated Lagrangian formulation, the axial linear and nonlinear normal strain increments are defined by:

$$\begin{cases}\Delta\varepsilon_z^{L} = \Delta w' - x\Delta u'' - y\Delta v'' \\ \Delta\varepsilon_z^{N} = (\partial\Delta U/\partial z)^2/2 + (\partial\Delta V/\partial z)^2/2 \\ \qquad = (\Delta u' - y\Delta\theta')^2/2 + (\Delta v' + x\Delta\theta')^2/2\end{cases} \tag{10}$$

in which, the superscripts L and N respectively denote the linear and nonlinear strain components, Δw is axial displacement increment of the cross-section, Δu, Δv is lateral displacement increments of the cross-section, $\Delta\theta$ is torsional deflection increment of the cross-section.

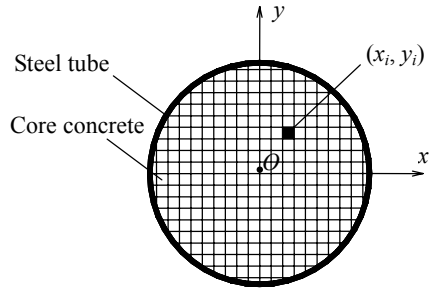

Fig.5 Fiber model of a CFST structure

As the influence of the lateral confined stresses are taken into account in the stress-strain curves of the concrete and steel tube, the axial strain increment of concrete $\Delta\sigma_{zc}(x, y)$ and steel tube $\Delta\sigma_{zs}(x, y)$ can be calculated approximately by the following Eq.(11):

$$\begin{cases}\Delta\sigma_{zc} = E_c(\varepsilon_z)\Delta\varepsilon_z^{L}(x,y) \\ \Delta\sigma_{zs} = E_s(\varepsilon_z)\Delta\varepsilon_z^{L}(x,y)\end{cases} \tag{11}$$

where $E_c(\varepsilon_z)$ is concrete tangent modulus, $E_s(\varepsilon_z)$ is steel tube tangent modulus.

The axial force N and bending moment M_x and M_y of the cross-section can then be obtained by the following Eq.(12):

$$\begin{cases}N = \int_A \sigma_z \mathrm{d}A \\ M_x = \int_A \sigma_z y \mathrm{d}A \\ M_y = -\int_A \sigma_z x \mathrm{d}A\end{cases} \tag{12}$$

Similar to the elastic beam theory, the shape function is introduced into the element, so that the increments can be denoted with the nodal displacement increments as Eq.(13):

$$\begin{cases}\Delta w = N_{w1}\Delta w_i + N_{w2}\Delta w_j \\ \Delta\theta = N_{w1}\Delta\theta_i + N_{w2}\Delta\theta_j \\ \Delta u = N_1\Delta u_i + N_2\Delta u_i' + N_3\Delta u_j + N_4\Delta u_j' \\ \Delta v = N_1\Delta v_i + N_2\Delta v_i' + N_3\Delta v_j + N_4\Delta v_j'\end{cases} \tag{13}$$

where N_{w1} and N_{w2} are the linear shape functions of axial deformation, N_1~N_4 are the cubic shape functions of bending deformation.

The end forces of the beam element *i-j* according to the nodal freedoms are given as Eq.(14):

$$\begin{cases} N_i = -(N_a + N_b)/2 \\ N_j = (N_a + N_b)/2 \\ Q_{yi} = -(M_{xb} - M_{xa})/L \\ Q_{yj} = (M_{xb} - M_{xa})/L \\ M_{xi} = -M_{xa} \\ M_{xj} = M_{xb} \\ Q_{xi} = (M_{yb} - M_{ya})/L \\ Q_{xj} = -(M_{yb} - M_{ya})/L \\ M_{yi} = -M_{ya} \\ M_{yj} = M_{yb} \end{cases} \tag{14}$$

where the end forces of member with subscript *a* and *b* are calculated from Eq.(12).

According to the virtual work principle and the element equilibrium condition, the element stiffness equation in the incremental form can be obtained as:

$$([\boldsymbol{K}_{\mathrm{ep}}]^{\mathrm{e}} + [\boldsymbol{K}_{\mathrm{G}}]^{\mathrm{e}})\{\Delta \boldsymbol{u}\}^{\mathrm{e}} = \{\Delta \boldsymbol{P}\}^{\mathrm{e}} \tag{15}$$

where $[\boldsymbol{K}_{\mathrm{ep}}]^{\mathrm{e}}$ and $[\boldsymbol{K}_{\mathrm{G}}]^{\mathrm{e}}$ are respectively the elastic-plastic stiffness matrix and geometric stiffness matrix considering the spreading of the plastic domain. The element displacement increment vector is given as:

$$\{\Delta \boldsymbol{u}\}^{\mathrm{e}} = [\Delta w_{\mathrm{i}}, \Delta u_{\mathrm{i}}, \Delta u'_{\mathrm{i}}, \Delta v_{\mathrm{i}}, -\Delta v'_{\mathrm{i}}, \Delta \theta_{\mathrm{i}}, \Delta w_{\mathrm{j}}, \Delta u_{\mathrm{j}}, \Delta u'_{\mathrm{j}}, \Delta v_{\mathrm{j}}, -\Delta v'_{\mathrm{j}}, \Delta \theta_{\mathrm{j}}]^{\mathrm{T}} \tag{16}$$

ULTIMATE BEHAVIOR OF CFST STRUCTURES USING DIFFERENT CONSTITUTIVE RELATIONSHIPS

In this paper, the applicability of the above constitutive relationships was verified by analyzing the ultimate behavior of the CFST structures. To enhance the objectivity of the study, the experiments by non-proponents of the above constitutive relationships are taken as the objects of calculation (Cai, 2003). Details of four groups of specimens with different slenderness ratios are listed in Table 1. Two experimental results are listed for each group. The yield strength of steel tube and the cube crushing strength of concrete obtained from the specimens were 400 MPa and 69 MPa, respectively.

To take into account the effect of specimen manufacturing errors, it is assumed that the initial column lateral deformation satisfies a half-wave sine function, and that the initial column deflection was 1/2000 of the height. In addition, it is assumed that the secondary modulus is 1% of the initial modulus, and the approximate evaluation of β_{t} and β_{c} is 1.0 for the steel tube.

The calculated and experimental results of the ultimate compressive bearing capacity of the specimens are shown in Table 1. It is clear that all the calculated results are on the safe side of the experimental results. It is also found that the results calculated from Eq.(3) are the closest to the experimental results correspondingly, although the difference in the results calculated by the different constitutive relationships is insignificant. The curves of the lateral deformation at the midpoint vs the compressive axial force of the tested CFST columns are shown in Fig.6. It was found that the failure behaviour calculated by the three constitutive relationships fit well the experimental results from an engineering point of view. As a result, it is suggested that any of the above three constitutive relationships can be used to estimate the failure behaviour of the CFST compressive members.

To test the variation of ultimate bearing capacity of the CFST arch rib structures based on the different constitutive relationships, the experiment described in Chen (2000) was taken as a comparison object. The span of the experimental model of CFST arch rib is 4600 mm. The inner curve of the arch rib is a second-

Table 1 Dimension and ultimate compressive bear capacity of the specimens

No.	Dimension of steel tube (mm)		Calculated results (kN)			Experimental results (kN)	
	D×*t*	*L*	Eq.(1)	Eq.(3)	Eq.(5)	No. 1	No. 2
G6	108×4.5	700	1074.2	1106.4	1079.6	1350	1200
G10	108×4.5	1130	977.1	1041.4	981.5	1100	1200
G15	108×4.5	1670	895.1	970.6	908.9	1000	1000
G20	108×4.5	2230	772.0	821.3	780.0	900	850

degree parabola, $Y=X^2/3.45$, and the net height is 1533 mm. The diameter and thickness of the steel tube is 76 mm and 3.792 mm respectively. The yield strength of the steel tube is 307.67 MPa, and the Young's modulus is 206×103 MPa. The cube crushing strength of concrete is 36.8 MPa, and the Young's modulus is 31×103 MPa. The vertical loading point locates on the quartile of arch rib span.

A comparison of the calculated results and the test results of the vertical deflection is shown in Fig.7a, showing that the failure behaviour based on the three different constitutive relationships are consistent and agree well with the test results, although the stress-strain relation of confined concrete is inconsistent when the compressive strain is large (Fig.7b).

APPLICATION OF THE PRESENT APPROACH IN STRUCTURAL DESIGN

As an example of applying the present approach for CFST arch bridges, half of an arch bridge is employed as shown in Fig.8, and the in-plane stability was examined. The span length of this CFST arch bri-

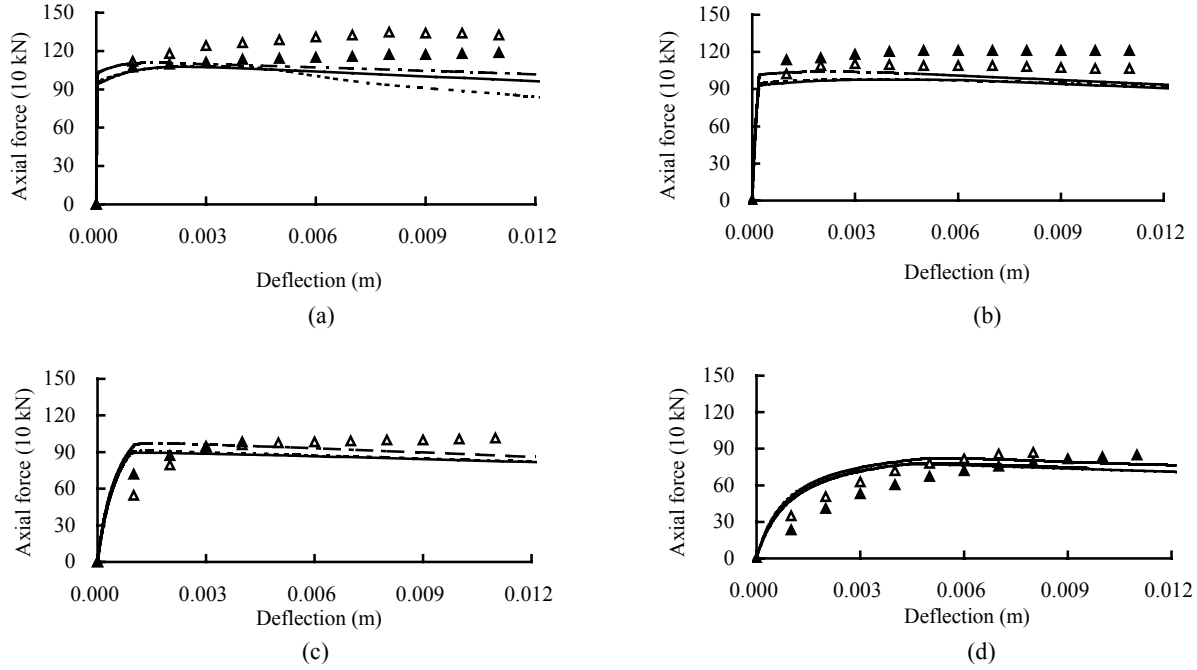

Fig.6 Load-displacement curve of CFST experimental column. (a) G6; (b) G10; (c) G15; (d) G20
——— Eq.(1); -·-·-·- Eq.(3); - - - - - - - Eq.(5); △ Exp.-1; ▲ Exp.-2

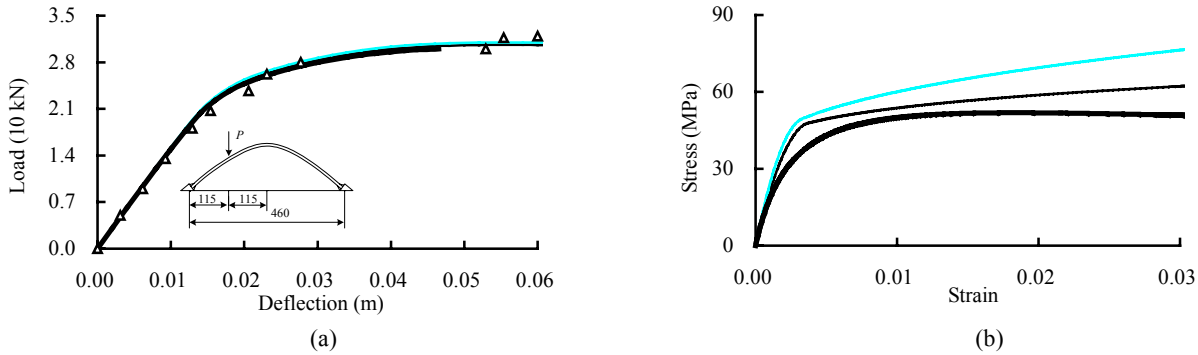

Fig.7 Comparison of ultimate bearing capacity of CFST arch rib structure
(a) Load-disp. curve on loading point; (b) Stress-strain relations of confined concrete
——— Eq.(1); ——— Eq.(3); ——— Eq.(5); △ Exp.

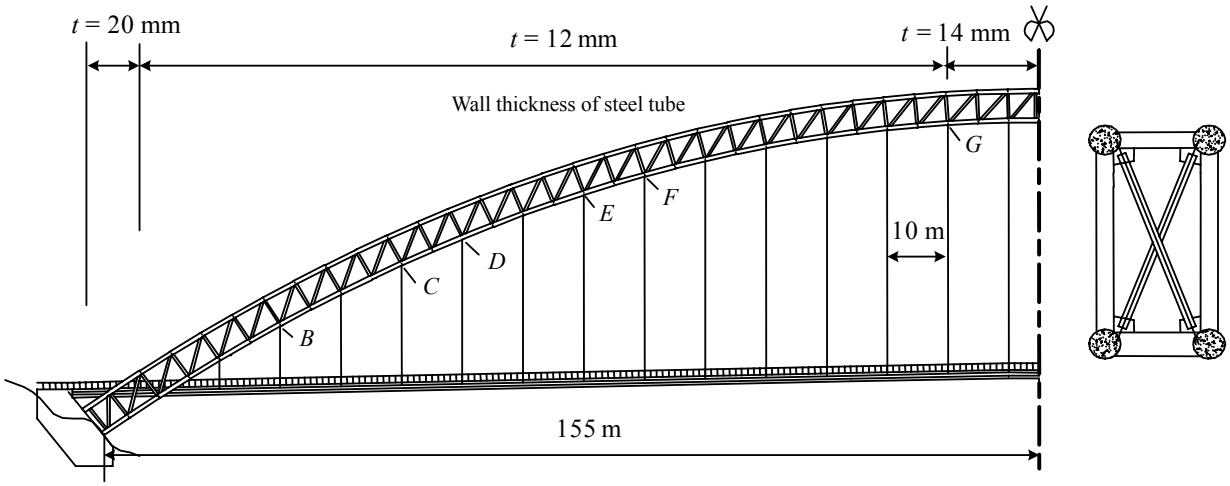

Fig.8 Side view and cross-section of braced CFST arch bridge

dge is 308 m, and the height is 56 m. The cross-section of the arch rib consists of 4×Ø850 mm steel tubes. The thicknesses of the steel tubes are 20 mm, 14 mm and 12 mm. The yield strength of the steel tube is 375 MPa (t=20 mm) and 390 MPa (t=12~14 mm) respectively. The cube crushing strength of the core concrete is 50 MPa. The distance between the upper and lower chords is 5.2 m. Steel pipes are employed as the braced members. The diameter and thickness of the steel pipes are 529 mm and 10 mm respectively.

To examine the in-plane stability of the arch bridge, half of the cross-section is modelled as shown in Fig.9. The live load acting location is considered so that the cross-sectional forces at 1/4 span length become max under traffic load. The dead load of the arch rib is taken into account by the analysis program automatically. Eq.(1) is used as the stress-strain relationship of confined concrete.

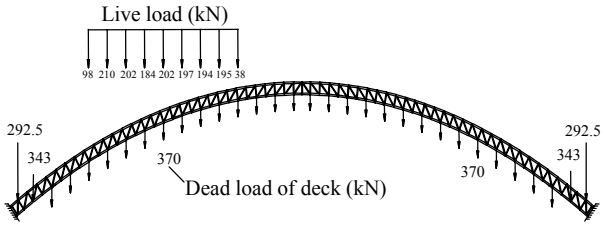

Fig.9 Analytical model and acting load

Fig.10 shows load-deflection curves of the lower chord. The locations of nodes B~G are shown in Fig.8. The results showed that the structure will become unstable when the load coefficient λ is near 2.86, i.e. the limiting strength of the arch rib in-plane is 2.86 times dead load and live load. In this figure, λ=1.0 means design load.

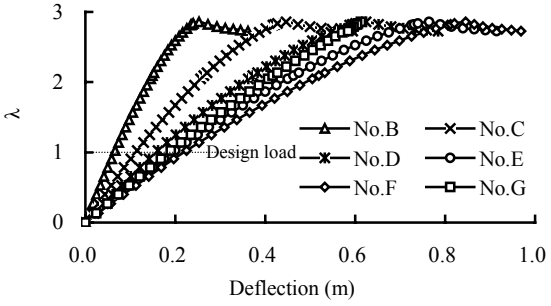

Fig.10 Load-deflection curves at node B~G

Fig.11 shows the deformations of the arch rib at: pre-buckling load (λ=2.13), buckling load (λ=2.86) and post-buckling load (λ=2.79). It is shown clearly that the buckling occurred in a member near the base, because the thickness of that steel tube is small and the axial force is larger. Therefore, special attention should be paid to the local buckling of members of the braced arch rib during structural design.

Geometric nonlinear behavior is also an important problem in the design of long span arch bridges. Because the bending moment increases with the deformation of the arch rib, the cross-sectional forces will be underestimated using linear analysis. To exa-

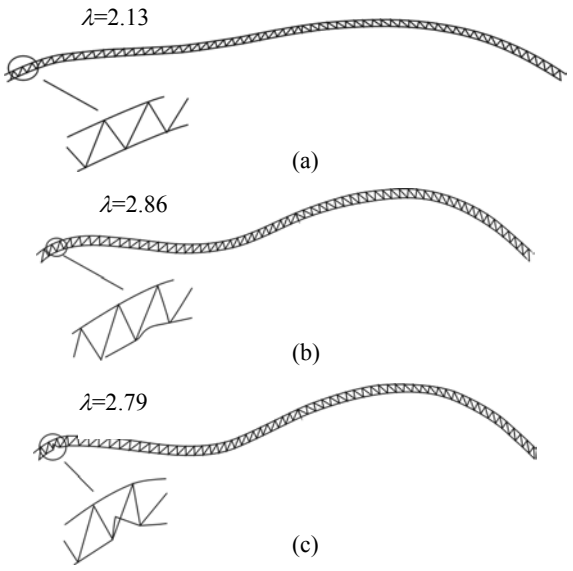

Fig.11 Deformations at: pre-buckling load (a), buckling load (b) and post-buckling load (c)

mine the influences of geometric nonlinearity, the deflection, axial force and bending moment of five cross-sections under the designed load are shown in Fig.12. In this figure, the deformation and the cross-sectional forces increase almost linearly with load coefficient λ. The effect of geometric nonlinearity is not significant.

CONCLUSION

The stress-strain relation of CFST structures is complex due to the combined influence of the confined concrete and outer steel tube. In this paper, an analytical approach for estimating the ultimate stabilizing bearing capacity of CFST structures is proposed considering material and geometric nonlinearity based on space beam theory. Three different constitutive relationships were investigated. The accuracy of using different constitutive relationships was examined by comparing the calculated and experimental results. A braced arch rib with span of 308 m was analyzed and the stability of the CFST arch bridges was examined. From the results, the following conclusions were reached:

1. The failure behaviour of CFST members and structures can be simulated accurately by the method presented.

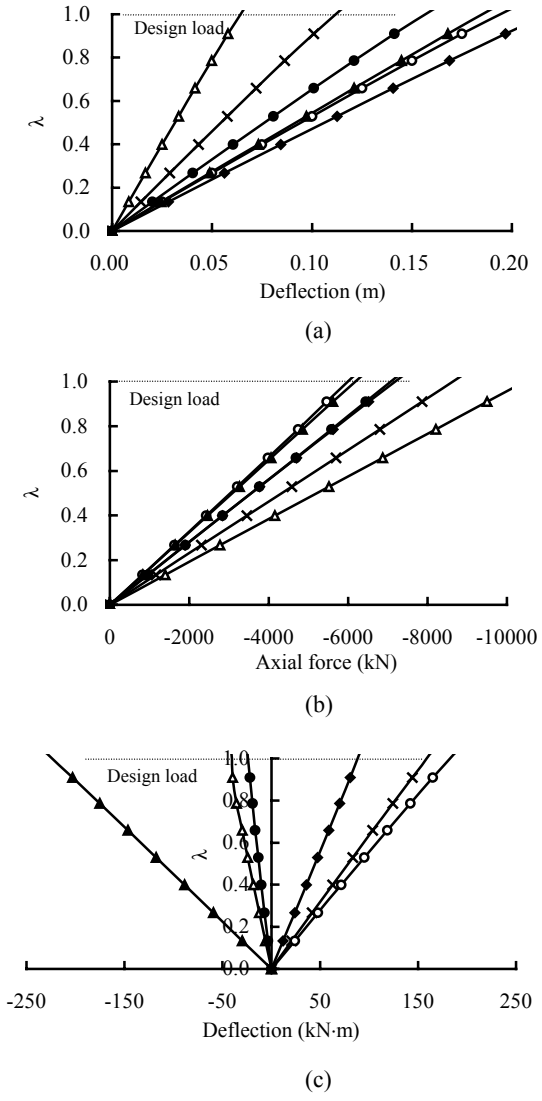

Fig.12 Deflection, axial force and bending moment under design load

(a) Load-deflection curve; (b) Load-axial force curve; (c) Load-bending moment curve

2. The influence of the different constitutive relationships of the confined concrete on the ultimate behavior is insignificant.

3. It is possible that local buckling of a member can occur in braced CFST arch bridges. To check buckling safety of CFST arch bridges accurately, an elastic-plastic large displacement analysis is necessary based on space beam theory.

4. The effect of geometric nonlinear behavior is insignificant when design loads are applied on long span braced CFST arch bridges.

References

Cai, S.H., 2003. Modern Steel Tube Confined Concrete Structures. China Communications Press, Beijing (in Chinese).

Chen, B.C., 2000. Experimental study on mechanic behaviors of concrete-filled steel tubular rib arch under in-plane loads. *Engineering Mechanics*, **17**(2):44-50.

Fujii, K., 2003. An analysis on Concrete Filled Steel Tubular circular column under cyclic horizontal loads. *Journal of Structural Engineering*, **49**:1041-1050 (in Japanese).

Han, L.H., 2000. Steel Tube Confined Concrete Structures. Science Press, Beijing (in Chinese).

Nosaki, K., 1996. Research on bending performance of steel tube confined concrete column. *Journal of Japan Concrete*, **18**(2):1289-1294 (in Japanese).

Pan, Y.G., 1989. The constitutive relationship of the core concrete in concrete filled steel tubes. *Journal of Harbin Architectural and Civil Engineering Institute*, **22**(1):37-47 (in Chinese).

Susantha, K.A.S., Ge, H.B., 2001. Uniaxial stress-strain relationship of concrete confined by various shaped steel tubes. *Engineering Structures*, **23**:1331-1347.

Tang, J.L., Hino, S.I., 1996. Modeling of stress-strain relationships for steel and concrete in concrete filled circular steel tubular columns. *Journal of Steel Structure*, **3**(11):35-46 (in Japanese).

Zhong, S.T., 1999. The Concrete-Filled Steel Tubular Structures. Heilongjiang Science and Technology Press, Harbin (in Chinese).